Electronic Excitations of Glycine, Alanine, and Cysteine Conformers from First-Principles Calculations

R. Maul,* M. Preuss, F. Ortmann, K. Hannewald, and F. Bechstedt

Institut für Festkörpertheorie und-optik, Friedrich-Schiller-Universität Jena, Max-Wien-Platz 1, 07743 Jena, Germany, and European Theoretical Spectroscopy Facility (ETSF)

The electronic and optical properties are studied for three conformers of amino acid molecules using gradient-corrected (spin-) density functional theory within a projector-augmented wave scheme and the supercell method. We investigate single-particle excitations such as ionization energies and electron affinities as well as pair excitations. By comparing eigenvalues resulting from several local and nonlocal energy functionals, the influence of treatment of exchange and correlation is demonstrated. The excitations are described within the Δ-self-consistent field method with an occupation number constraint to obtain excitation energies and Stokes shifts. The results are used to also discuss the optical absorption properties. In contrast to the lowest single- and two-particle excitation energies, remarkable changes are found in absorption spectra in dependence on the conformation of the molecule geometry.

I. Introduction

Properties of isolated molecules, such as amino acids, are fundamental to the understanding of complex structures such as proteins in biological materials or even in novel electronic and optoelectronic devices based on or modified by molecular species. Many biological phenomena can be traced back to fundamental properties of molecular constituents. This holds for several processes such as signal exchanges, which are accompanied by electronic excitations. In addition to their biological significance,[1] there are applications of peptides, consisting of amino acids, in molecular electronics[2] or in functionalization of semiconductor quantum dots[3,4] and carbon nanotubes.[5−7] The understanding of the electronic properties of amino acid molecules arranged in short peptide chains[8,9] may be one key to future nanotechnology applications such as those based on molecular transport.[10] A theoretical interpretation of such phenomena can be related to the excitation energies of the building blocks of peptides, for example, the amino acids.[11]

Among the 20 α-amino acids, glycine, alanine, and cysteine play outstanding roles as model systems because of the smallness of the corresponding molecules. Their principal structure $NH_2-CH(R)-COOH$ contains a carbon backbone with a carboxyl group (COOH), an amino group (NH_2), and a varying organic side group (R) linked to a central, tetrahedrally coordinated carbon atom (C_α). The side group increases from R = H (glycine), to R = CH_3 (alanine), and to R = CH_2-SH (cysteine). In solution, the acidic and basic groups may react with each other forming a zwitterion, which also occurs in crystalline phases. The chemical and physical properties of the gas-phase species depend on the molecular geometry of a given amino acid. Conformers occur because of the rotational degrees of freedom. The molecule with the smallest side group, glycine, can be divided into the rigid fragments NH_2, CH_2, CO, and OH. Then, three rotational degrees of freedom are related to the

connecting bonds C−N, C−C, and C−O, respectively. For instance, in the glycine case, there are two possible angles for each bond rotation to achieve a planar (p) heavy atom arrangement resulting in eight conformers with C_s symmetry. However, in addition, nonplanar (n) structures are formed by distortion of planar conformers. Thereby, the carboxyl group can be arranged in a *cis* or *trans* position. The geometries and the energetics of such conformers have been intensively studied by total energy calculations (see refs 12−18, 22, and references therein). The predictions of stability, bond lengths, and bond angles are based on various quantum chemistry studies, for example, on the Møller−Plesset (MP2) perturbation theory level[23] or calculations within the density functional theory (DFT).[24,25]

Studies of the electronic excitations of the amino acids glycine, alanine, and cysteine are rather rare. Gas-phase properties of amino acids, mainly of glycine and alanine, have been investigated experimentally using electron momentum spectroscopy,[26] resonant two-photon ionization,[27] and photoelectron spectroscopy (PES).[28] Data on alanine have also been obtained from previous HeI photoelectron spectra.[29−31] Recently, vertical attachment energies for the formation of low-lying temporary anion states have been measured by, for example, electron transmission spectroscopy for glycine and alanine.[32,33] Ionization potentials and electron affinities of the most stable glycine conformers have been studied in several papers in the framework of DFT using hybrid exchange-correlation (XC) functionals and Gaussian basis sets.[34−36] Calculations of this type have been performed for many conformers not only for glycine but also for alanine.[37] For the computation of pair excitation energies, coupled cluster (CC) methods[23] have been applied.[38]

In the present paper, we present and discuss calculated single-particle and pair excitation energies of the most favorable conformers of glycine, alanine, and cysteine molecules. They are computed in the framework of DFT and the Δ-self-consistent field (ΔSCF) method.[39,40] For the purpose of further applications, for example, the study of molecule−substrate interactions, an approach that is also applicable to bulk materials, is chosen.

* To whom correspondence should be addressed. Permanent address: Institut für Nanotechnologie, Forschungszentrum Karlsruhe, Hermann-von-Helmholtz-Platz 1, 76344 Eggenstein-Leopoldshafen, Germany.

First-Principle Calculations of Electronic Excitations

J. Phys. Chem. A, Vol. 111, No. 20, 2007 **4371**

The molecules are described within repeated supercells,[41] and the single-particle eigenfunctions are represented within the projector-augmented wave (PAW) method.[42–44] The influence of the XC functional and the actual molecule geometry is also studied. The results are compared with available experimental and theoretical data.

II. Methods

The employed DFT[24,25,39] code is the Vienna Ab initio Simulation Package (VASP).[45] The electron–ion interaction is modeled by PAW pseudopotentials.[42,43] The Kohn–Sham (KS) equation[25] is solved for the valence electrons for a given XC functional. The resulting all-electron PAW functions are expanded in plane waves in the regions between the cores. Plane waves up to a kinetic energy cutoff of 37 Ry give converged results with respect to the total energy.[22] Exchange and correlation are generally treated in a semilocal approximation of DFT within the generalized gradient approximation (GGA) according to Perdew and Wang (PW91).[46,47] Apart from a few exceptions, it is well-suited to describe the energetics, geometries, and vibrational spectra of glycine, alanine, and cysteine.[22] Nevertheless, for selected quantities such as energy gaps, we study the influence of the XC treatment by using hybrid functionals. The PBE0 functional[48] developed by Perdew, Burke, and Ernzerhof (PBE) combines the generalized gradient-corrected PBE XC functional with a predefined amount of exact exchange. Practically, 25% of the exchange is replaced by the Fock operator. Another hybrid functional HSE goes back to Heyd, Scuseria, and Ernzerhof.[49] It contains a screened Coulomb potential in the exchange term. The Coulomb potential $\sim 1/|x|$ in the exchange term is replaced by a screened potential erfc-$(\mu|x|)/|x|$ with a Thomas–Fermi-like screening parameter $\mu = 0.3$ Å^{-1}. For comparison, we employ the local density approximation (LDA)[50] as well. Single-particle excitation energies are also studied within a spin-polarized GGA version.

Because of the plane-wave expansion, we employ Born–von Karman boundary conditions and study a periodic arrangement of simple cubic supercells each containing one molecule. The supercell must be sufficiently large to avoid the interaction of a molecule with its images in adjacent cells.[51] Therefore, we use supercells up to edge lengths of 22 Å. Our criterion for noninteracting molecules is a band structure that is almost free of band dispersion. Consequently, the summation over the Brillouin zone in the total energy and electron density expressions is restricted to the zone center Γ.

The KS eigenvalues of DFT do not account for neutral or charged excitations of the molecule. Therefore, their differences to the vacuum level or between empty and occupied levels usually underestimate single-particle or two-particle excitation energies. Within a Green's function approach, one has to take into account self-energy effects.[51] However, the localization of the electron states in a molecule allows for a numerically less demanding treatment of the many-body effects by the ΔSCF method[39,40]—also called occupation-constrained DFT calculation. Thereby, the total energy differences (here, mostly in spin-polarized DFT–GGA) between the N-electron ground state and the excited states of the molecules, for example, with $(N-1)$ or $(N+1)$ electrons, are computed. The lowest single-electron excitations are the (first) ionization potential (IP)

$$\text{IP} = E(N-1) - E(N) \tag{1}$$

and the electron affinity (EA)

$$\text{EA} = E(N) - E(N+1) \tag{2}$$

Here, the ionized molecules with one missing or additional electron are characterized by the total energies $E(N-1)$ and $E(N+1)$, respectively, computed for the geometry of the N-electron ground state of one and the same conformer of the neutral molecule. Without geometry changes, one also calls the energies (1 and 2) vertical IPs or EAs.[34,37,38] In addition, structural relaxation can be taken into account. We indicate the resulting geometries of the $(N-1)$ or $(N+1)$ systems by an asterisk. They lead to the corresponding adiabatic quantities IP* and EA*. The EA is also a measure of the energy gained in the transformation process from a neutral molecule and an electron into a negatively charged ion. In the opposite case, when energy is needed, one speaks about (vertical) attachment energy for the formation of a low-lying anion state of an amino acid molecule.[32,33]

To accelerate the convergence of the total energies for the cationic $(N-1)$ and anionic $(N+1)$ electronic systems with the supercell size, we have added correction terms to compensate at least for the monopole and dipole moments.[19,20]

The HOMO–LUMO gap energy is defined as the difference of the KS eigenvalues for the LUMO, $\epsilon_{\text{LUMO}}^{\text{KS}}$, and the HOMO, $\epsilon_{\text{HOMO}}^{\text{KS}}$:

$$E_{\text{pair}}^{\text{KS}} = \epsilon_{\text{LUMO}}^{\text{KS}} - \epsilon_{\text{HOMO}}^{\text{KS}} \tag{3}$$

In a two-particle picture, we combine the EA and IP to calculate the lowest pair energy of a molecular system

$$E_{\text{pair}}^{\text{QP}} = \text{IP} - \text{EA} \tag{4}$$

In extended nonmetallic systems, this expression defines the so-called quasiparticle (QP) gap.[40,51] It contains the effects of the electronic relaxation, for example, the renormalization to a QP, in the presence of an isolated additional electron and of an isolated hole.

Neglecting spin effects, the true lowest pair excitation energy, $E_{\text{pair}}^{\text{ex}}$, of the system can also be defined within the ΔSCF method or occupation-constrained DFT according to

$$E_{\text{pair}}^{\text{ex}} = E(N, e+h) - E(N) \tag{5}$$

where $e+h$ indicates the presence of an electron–hole pair. The calculation of the total energy, $E(N, e+h)$, is done by applying the occupation constraint that the HOMO contains a hole and the excited electron resides in the LUMO. In addition to the QP effects, the energy $E(N, e+h)$ also contains excitonic effects, that is, the (screened) electron–hole attraction and the (unscreened) electron–hole exchange interaction.[51] The pair energy (expression 5) may be measurable in an optical absorption experiment. In an optical emission experiment, a smaller pair energy, $E_{\text{pair}}^{\text{ex}*}$ is detected, if the lattice of the molecular system has enough time to relax to the presence of the electron–hole pair. Then, the molecule geometry of the excited state, indicated by the asterisk, is different from the ground-state geometry. The structural changes give rise to the Stokes shift

$$\Delta_{\text{Stokes}} = E_{\text{pair}}^{\text{ex}} - E_{\text{pair}}^{\text{ex}*} \tag{6}$$

of the pair excitation between absorption and emission lines.

The optical absorption of a system may be characterized by the imaginary part of the dielectric function $\epsilon(\omega)$. Despite the anisotropy of an amino acid molecule, here, we discuss only a spatial average of the resulting dielectric tensor. For a gas of molecules, only a spatial average should be detectable, even
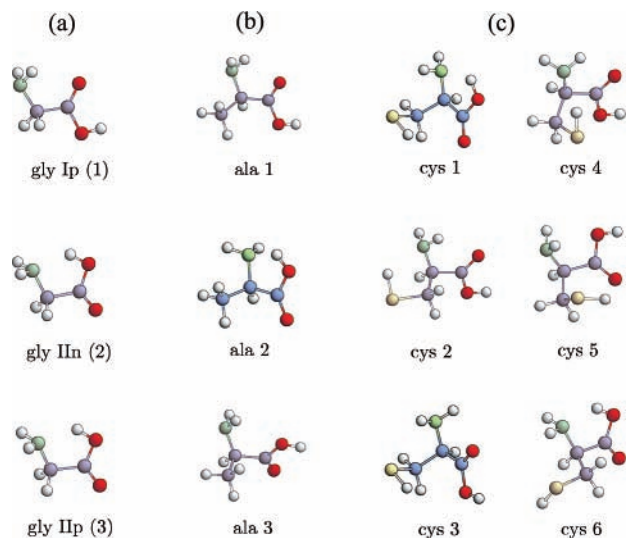
Figure 1. Three most favorable conformers of glycine (a), alanine (b), and cysteine (c). In the cysteine case, an additional three conformers are shown. Different atoms are indicated by different colors: carbon (blue), oxygen (red), nitrogen (green), sulfur (yellow), and hydrogen (white).

using linearly polarized light. With the eigenstates $|\lambda\rangle$ and eigenvalues ϵ_λ^{KS} of the KS equation, this average reads as[21]

$$\text{Im } \epsilon(\omega) =$$

$$\left(\frac{2\pi e\hbar}{m}\right)^2 \frac{1}{3} \sum_{\alpha=x,y,z} \frac{2}{\Omega} \sum_{\lambda,\lambda'} \frac{|\langle\lambda\,|\,\hat{p}_\alpha\,|\,\lambda'\rangle|^2}{(\epsilon_\lambda^{KS} - \epsilon_{\lambda'}^{KS})^2} [n_{\lambda'} - n_\lambda]$$

$$\delta\,(\epsilon_\lambda^{KS} - \epsilon_{\lambda'}^{KS} - \hbar\omega) \quad (7)$$

with the level occupation numbers n_λ, the α-th Cartesian component of the momentum operator $\hat{p}_\alpha$, and the cell volume Ω. QP renormalization and excitonic effects are neglected in expression 7. However, at least their influence on the peak positions can be taken into account if the energy differences $(\epsilon_\lambda^{KS} - \epsilon_{\lambda'}^{KS})$ in the spectral function are replaced by pair excitation energies that are computed according to expression 5.

III. Results and Discussion

A. Ionization Potentials and Electron Affinities. In a previous paper, we have investigated the energetics, geometry, and molecular vibrations of a total of 38 conformers—13 for glycine, 10 for alanine, and 15 for cysteine—in the framework of DFT−GGA.[22] The results were in good agreement with quantum chemical calculations.[14,17,18] Only conformers with a hydrogen bridge bond O−H···N gave slightly different results. The geometries of the most stable conformers in our DFT description agreed with the most stable structures found by quantum chemists. There was only a variation in their ordering with reference to the total energy. For that reason, we restrict ourselves in the following to the generally accepted three most stable conformers of each amino acid, which are shown in Figure 1. The atomic geometries calculated for the ground state are used to determine the vertical single-particle excitation energies (1 and 2).

The resulting vertical ionization energies are listed in Table 1 and compared with results of other calculations using DFT with hybrid functionals or many-body perturbation theory, for example, B3LYP/6-31G** and MP2/6-311++G**,[28] P3 ap-

proximation of electron propagator theory with the 6-311G** basis set,[35] as well as outer valence Green's function (OVGF) method, MP2 or QCISD level.[37] Considering the completely different methods used to account for exchange and correlation and different details of their implementation, for example, different basis sets, one can state an excellent agreement. With a few exceptions, the deviations are of the order of 2%. The influence of the conformers on the ionization energies is small, for example, for glycine and alanine smaller than 0.1 eV. The effect is somewhat larger for cysteine in agreement with the geometric changes shown in Figure 1. In the average over different conformers and methods, one finds IP = 9.9 (glycine), 9.7 (alanine), and 8.9 eV (cysteine). At least, in the glycine case, the average value is in complete agreement with the ionization energy of 10.0 eV measured by means of PES.[29,30] We also checked the influence of the spin polarization after excitation. However, the results of the DFT−GGA with and without spin polarization did not change very much. Spin polarization reduces the ionization energies by about 0.24 (glycine), 0.21 (alanine), and 0.12 eV (cysteine).

According to expression 2, we computed positive vertical electron affinities in the range of 0.29−0.39 eV for the nine conformers under consideration. Spin polarization also reduces these values further by about 0.10 (glycine), 0.14 (alanine), and 0.03 eV (cysteine). Electron attachment into the empty π^* orbital of the −COOH group, at least a temporary occupation, was observed for glycine and alanine.[32,33] However, to the best of our knowledge, the glycine molecule does not form a valence type anion in the gas phase on a longer time scale.[52] Probably, the binding of an excess electron considerably stabilizes the zwitterion of glycine relative to the nonzwitterion form. We cannot exclude that our result of a small but positive EA is a consequence of the use of a local or semilocal (here, GGA) approach to exchange and correlation. The localization of empty orbitals close to the vacuum level is generally overestimated in GGA.[51] Taking into account the excitation aspect in the form of self-energy or changing to hybrid functionals, which include partly the spatially nonlocal Fock exchange, there is always a level shift toward higher energies accompanied by the tendency for delocalization (see the discussion in ref 51).

This trend is illustrated in Figure 2 for the six most stable conformers of cysteine shown in Figure 1c. In this figure, the eigenvalues of the KS[25] or generalized KS equation[53] are plotted for the HOMO and LUMO states with respect to the vacuum level. The nonlocality of the XC functional has a strong influence on the energetical positions. The nonlocality increases along the row LDA, GGA, HSE, and PBE0. The sequence of LDA and GGA is clear from the definition and also the stronger nonlocality of HSE and PBE0 because of partial inclusion of exact exchange. Thereby, the effect is stronger in PBE0 than in HSE. This is due to the assignment of a screened Hartree−Fock exchange in HSE, whereas PBE0 includes undamped long-range Hartree−Fock exchange. With a rising amount of nonlocality, the LUMO state is shifted toward the ionization edge and, hence, becomes more delocalized. The lowest orbital energies occur in the framework of LDA or GGA while the PBE0 functional leads to the strongest delocalization. Figure 2 shows the opposite trend for the HOMO states. Their binding energies increase with the nonlocality. As a consequence, the HOMO−LUMO gap energy (expression 3) is drastically increased by about 1.5 eV (HSE) or 2.5 eV (PBE0) with respect to the LDA/GGA values, which are very similar. An inclusion of Hartree−Fock eigenvalues computed with the complete nonlocal exchange term would lead to much more separated

First-Principle Calculations of Electronic Excitations

J. Phys. Chem. A, Vol. 111, No. 20, 2007 **4373**

TABLE 1: Calculated Vertical Ionization Energies for the Three Most Stable Conformers of Glycine, Alanine, and Cysteine[a]

amino acid	conformer	present DFT-GGA	ref 37			ref 28		ref 35
			OVGF	MP2	QCISD	B3LYP	MP2	P3
glycine	Ip	9.74 (9.52)	9.82					9.9
	IIn	9.81 (9.57)	9.98					10.0
	IIp	9.79 (9.55)						9.6
alanine	1	9.53 (9.33)	9.67	9.75	9.46	9.58	9.51	
	2	9.57 (9.36)	9.85	10.20	9.67	9.78	9.68	
	3	9.61 (9.40)				9.72	9.77	
cysteine	1	9.06 (8.93)	9.21					
	2	8.74 (8.59)	8.66					
	3	8.84 (8.75)						

[a] Results including spin-polarization effects are given in parentheses. They are compared with results of other calculations using different methods.[28,35,37] All values are in eV.
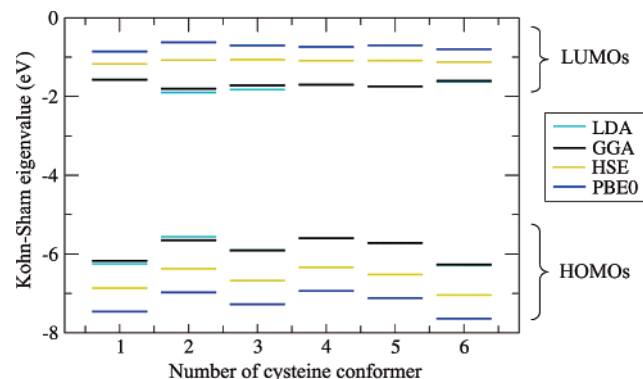

Figure 2. KS eigenvalues of the HOMO and LUMO states with respect to the vacuum level for the six most stable cysteine conformers described in Figure 1c. Results for four different XC functionals of DFT are given as follows: LDA (green), GGA (black), PBE0 (blue), and HSE (yellow).

TABLE 2: Lowest Pair Excitation Energies (3−5) and Stokes Shifts (6) of Glycine, Alanine, and Cysteine Conformers in Figure 1[a]

amino acid	conformer	absorption			emission	
		E_{pair}^{KS}	E_{pair}^{QP}	E_{pair}^{ex}	$E_{pair}^{ex}*$	Δ_{Stokes}
glycine	Ip	4.60	9.45	5.51	5.18	0.33
	IIn	4.70	9.43	5.38	4.48	0.90
	IIp	4.70	9.41	5.44	5.16	0.28
alanine	1	4.54	9.22	5.36		
	2	4.58	9.19	5.15		
	3	4.34	9.25	5.37		
cysteine	1	4.60	8.67	4.94	3.77	1.17
	2	3.85	8.39	4.70	3.55	1.15
	3	4.19	8.42	4.87	3.53	1.34

[a] All values are in eV.

eigenvalues. This is in agreement with the influence of spatial nonlocality as discussed above. The HSE or PBE0 values of E_{pair}^{KS} should come close to the lowest true QP pair energies (expression 4) without excitonic effects. For nonmetallic crystals, these functionals, especially HSE, give values for the fundamental gaps that are close to those obtained within the many-body perturbation theory.[53−55]

B. Electron−Hole Pair Excitations. The discussion of the HOMO−LUMO gaps in section III.A leads directly to the lowest pair energies of the studied amino acids. Values calculated for the ground-state geometry (E_{pair}^{ex}) and those for the excited-state geometry ($E_{pair}^{ex}*$) are listed in Table 2 together with their differences, Δ_{Stokes}, the Stokes shifts due to the ionic relaxation in the presence of an excited electron−hole pair. For the purpose of comparison, excitation energies without excitonic effects (E_{pair}^{QP}) and without both excitonic and

QP effects (E_{pair}^{KS}) are also given. For all conformers of the amino acids, the comparison of the values E_{pair}^{QP} and E_{pair}^{ex} indicates extremely large excitonic binding energies of about 4.0 (glycine), 3.9 (alanine), and 3.7 eV (cysteine). Another interesting comparison shows that the KS gaps E_{pair}^{KS} in DFT− GGA quality are only somewhat smaller than the vertical excitation energies E_{pair}^{ex}. This indicates an almost cancellation of excitonic effects, corresponding to a redshift, and QP effects, corresponding to a blueshift. This observation has also been made for other molecular systems.[41,51,56]

The vertical pair excitation energies in Table 2 calculated for the ground-state geometry show similar trends as the vertical IPs in Table 1. Their variation with the conformer is below 0.2 eV. There is a less pronounced chemical trend along the row glycine, alanine, and cysteine with averaged energies 5.4, 5.3, and 4.8 eV. The presence of the thiol group in cysteine reduces the bonding of the electron in the HOMO considerably. Our values are somewhat smaller than results of the CC method with an augmented correlation consistent with the used basis set.[38] The comparison with these results indicates that the details of the correlation treatment may be important for the exact value of the excitation energy. However, for glycine, only the conformer Vn (in denotation of ref 22) was investigated in ref 38 while for alanine the most stable geometry has been studied.

The emission properties depend very much on the amino acid and its actual conformation in the excited state, that is, in the presence of an excited electron−hole pair. The influence of the excitation on the geometry is indicated in Figure 3 for the three most stable conformers of the discussed amino acids. These structural changes have a considerable influence on the excitation energy measurable in an emission experiment and the resulting Stokes shift (expression 6) with respect to the pair excitation energy (expression 5) detectable in optical absorption. This is already observable from glycine results in Table 2. The planar conformers Ip and IIp are rather stable and exhibit minor changes of the geometry after optical excitation. Only the H−N−C bond angle is somewhat increased. The pair energies $E_{pair}^{ex}*$ are only reduced by a Stokes shift of about 0.3 eV. The nonplanar structure IIn is more flexible. The O atoms and the H atom of the carboxyl group are more displaced out of their primary positions. As a consequence, the lowest pair excitation energy is drastically reduced by a Stokes shift of about 0.9 eV.

The two other amino acids under consideration are much more influenced by electron−hole excitations. This fact has been directly proven by computer experiments, more precisely by allowing ionic relaxation of the ground-state geometry in the presence of the neutral excitation of an electron−hole pair. Bringing the Hellmann−Feynman forces acting on every atom to vanish, final equilibrium geometries arise for the excited state.
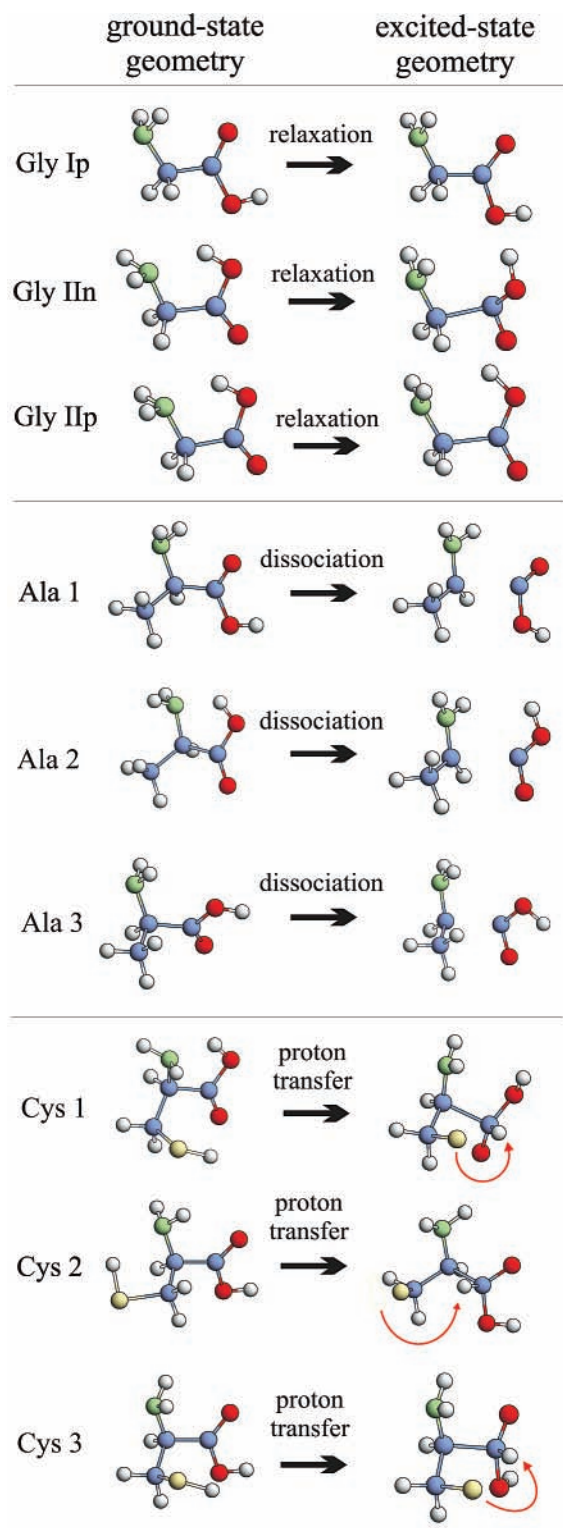
Figure 3. Changes of geometries of amino acid molecules due to electron–hole pair excitation.

Figure 4. Isodensity representation of HOMO (red) and LUMO (blue) orbitals for the most stable conformers of (a) glycine, (b) alanine, and (c) cysteine.

These geometries differ completely from the starting ones for alanine and cysteine. In the case of alanine, we observe (photo)-dissociation of all conformers as schematically indicated for the first three conformers in Figure 3. The carboxyl group is separated from the C_α carbon atom forming the chirality center. The (photo)ionization process is not hampered by an energy barrier. The cysteine conformers do not dissociate. Rather, a rearrangement of the atoms occurs. The optical excitation induces an intramolecular proton transfer. During the ionic relaxation, the H atom originally bonded to the sulfur atom of
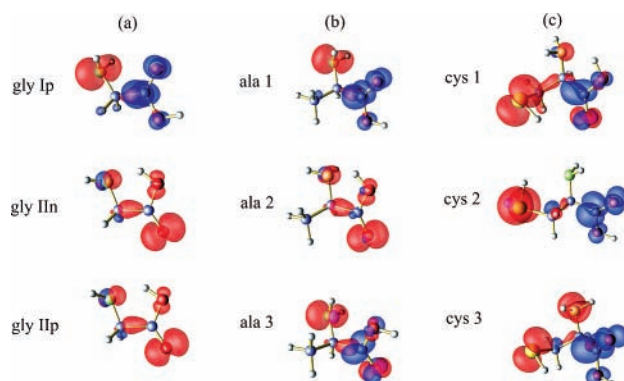
the side group migrates to the C atom of the neighboring carboxyl group. This reorganization process also occurs without an energy barrier. The resulting conformer with the protonated carboxyl group should present a short-lived molecule. Indeed, fluorescence decay measurements of tautomeric species due to excited-state intramolecular proton transfer show lifetimes of the order of 5 ns.[57] The proton transfer leads to a more drastic reduction of the lowest emission energies of cysteine conformers accompanied by a large Stokes shift of 1.2–1.3 eV. The huge shifts of about 25% of the absorption excitation energy make cysteine conformers to model systems to study the proton transfer in excitation spectroscopies. Proton transfer reactions are elementary steps in many enzymatic processes such as, bacterial photosynthesis and ATP synthesis.[58] Pump–probe experiments with a combination of IR and UV lasers may help one to study such chemical conversions[59,60]

C. Character of the Electron and Hole Orbitals. The KS orbitals of the LUMO and HOMO are presented in Figure 4 for ground-state geometries of the studied conformers. Despite only minor variations of the single-particle excitation energies in Table 1 with the conformer of an amino acid, they show that the chemical character of these orbitals may change significantly depending on the conformation. The two types I and II of glycine conformers (see Figure 1a) differ with respect to the position of the hydrogen atoms of the amino group and the H atom of the carboxyl group. Independent of the planarity of the molecule, according to Figure 4a, the conformers IIn and IIp possess a HOMO, which mainly consists of nonbonding lone pairs on the carboxylic oxygen atoms, in agreement with other findings.[37,38] However, there are also contributions from the σ bonding orbital between the two central carbon atoms C_α–C and a lone pair at the N atom. The corresponding contributions to the LUMO are mainly localized at the N and C_α atoms. There are no contributions from antibonding π orbitals of the C–O bonds.[38] For the glycine conformer Ip without a O–H···N hydrogen bridge bond, the situation is different. The HOMO mainly consists of a π orbital at the N atom of the amino group and a σ bonding orbital along C_α–C while the LUMO exhibits strong contributions from the two antibonding states of the carboxylic C–O and C=O bonds somewhat modified by contributions around the H atoms bonded to C_α.

Also, the alanine conformers (Figure 4b) are distinguishable into two groups. The HOMOs and LUMOs of conformers 1 and 3 are similar. The HOMO is dominated by a π lone pair orbital at the nitrogen atom. In the case of conformer 3, one observes in addition contributions from states localized at the C_α–C bond and O atoms. The LUMO is predominantly defined by antibonding C–O states. Such features have also been

First-Principle Calculations of Electronic Excitations

J. Phys. Chem. A, Vol. 111, No. 20, 2007 **4375**

observed in other calculations[28,37] but with less clarity. The conformer 2 shows a pronounced HOMO with lone pair contributions from the O and N atoms and a σ bonding $C_\alpha-C$ contribution. The LUMO with probability at C, N, and two O is less clearly pronounced. The remarkable difference in the electronic states of the conformers might be traced back to the presence of the bridge bond O−H···N in conformer 2.

The character of the LUMO and HOMO states of the cysteine conformers in Figure 1c (upper part) is influenced by the position of the S atom. Consequently, conformers 1 and 3 exhibit similarities. Their HOMO is dominated by a π lone pair orbital at the sulfur atom with additional contributions from the N atom of the amino group and to a smaller extend from oxygen atoms (see Figure 4c). This is (besides $C_\alpha-C$ contributions) also mentioned in ref 37. The HOMO of conformer 2 is more localized at the S atom of the side group. The LUMOs of all cysteine conformers are dominated by antibonding C−O states.

The comparison of the HOMO and LUMO states for the three amino acids shows that they have the tendency to be well-separated spatially for alanine. Especially, alanine 1 (Figure 4b) indicates this clear spatial separation of electron and hole after excitation, a fact that may be identified above as a possible driving force toward photoionization of the alanine conformers. Furthermore, this comparison shows the influence of the side group (R) on the orbitals characterizing the highest occupied and the lowest unoccupied molecule states. The carboxyl group in glycine IIn, IIp and alanine 2 is arranged in the *trans* position, which permits the O−H···N hydrogen bond. This structural similarity leads to similar distributions of the HOMOs and LUMOs in these conformers. In this respect, the displacement of the side group from R = H (glycine) to R = CH_3 (alanine) is of minor importance. The same effect is observable for glycine Ip, alanine 1, and alanine 2 where the carboxyl group is in the *cis* position. Substituting the side group by the thiol group R = CH_2SH (cysteine) reduces the dependence of the electron hole orbitals on the actual molecular geometry. For the cysteine conformers, Figure 4c shows that the occurrence of the O−H···N hydrogen bond has a minor influence on the distribution of the HOMOs and LUMOs.

D. Optical Absorption. The imaginary parts of the frequency-dependent dielectric function are shown in Figure 5 for the nine conformers of amino acids studied here in detail (cf. Figure 1). Apart from a prefactor linear in the frequency, they illustrate the optical absorption expected for amino acids in gas phase. We have restricted ourselves to the independent particle approximation (10). QP and excitonic effects are not taken into account. Apart from possible additional satellite structures, we expect that in experimental spectra the peaks are shifted by 0.4−0.9 eV (according to Table 2) toward higher photon energies because of the net many-body effects. The oscillator strengths may also be somewhat influenced by Coulomb enhancement due to electron−hole attraction. The coupling to molecular vibrations computed, for example, in ref 22 and hence a broadening of the absorption lines due to multiphonon processes, have also been disregarded. Nevertheless, despite the methodological limitations of our study, the spectra given in Figure 5 already give important information about peak positions and intensities. In particular, the spectra allow for a discussion of the conformer influence on the optical absorption.

In agreement with the discussion of the orbital contributions in Figure 4, the spectra of glycine conformers IIn and IIp are similar while that of Ip differs considerably. The absorption onset of glycine conformers is governed by optical transitions from the HOMO level into the LUMO, LUMO + 1, and LUMO
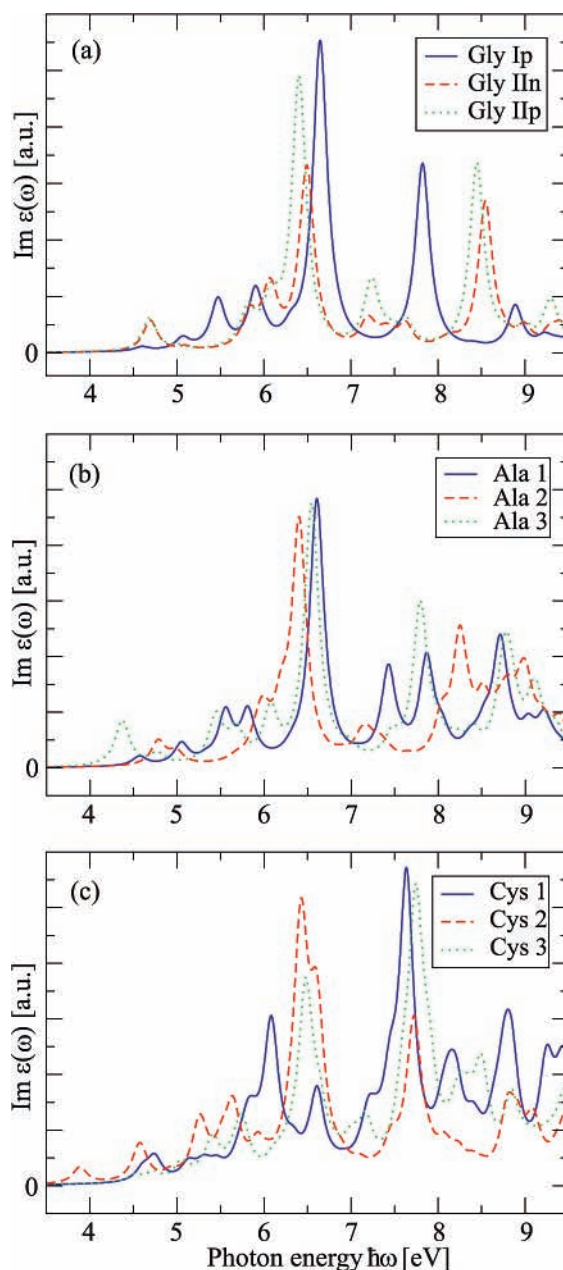

Figure 5. Optical absorption spectra of gas-phase molecules (a) glycine, (b) alanine, and (e) cysteine in the independent-particle approach. The imaginary part of the dielectric function Im $\epsilon(\omega)$ is shown for the three most stable conformers. They are represented by blue-solid (conformer 1), red-dashed (conformer 2), and green-dotted (conformer 3) lines. A lifetime broadening of 0.1 eV has been applied.

+ 2 states. However, the HOMO−LUMO transition is weak for Ip, whereas the oscillator strengths for HOMO → LUMO + 1 and HOMO → LUMO + 2 increase. The conformers of type II exhibit the opposite behavior. Only the HOMO−LUMO peak is really visible. Large deviations also occur for higher photon energies, for example, for the highest peaks around $\hbar \approx 6.5$ eV. The strongest peaks for the planar molecules Ip (IIp) at 6.7 eV (6.3 eV) are related to different optical transitions HOMO − 2 → LUMO (HOMO − 1 → LUMO + 1). The higher energy region of the optical spectra shows a significant conformational influence. Whereas the HOMO − 3 → LUMO transition is favored in glycine Ip, leading to a strong peak at 7.8 eV, we find dominating peak intensities at 8.4 and 8.5 eV in the higher frequency region for glycine IIn and IIp,

respectively. In both cases, the peaks are related to HOMO − 4 → LUMO + 1 transitions.

The absorption spectra of the alanine conformers in Figure 5b show more peaks as a consequence of the more complex side group. At the absorption edge, alanines 1 and 2 exhibit only weak HOMO−LUMO transitions, a fact that is finally a consequence of the spatial separation of the corresponding orbitals. A stronger spatial overlap of the HOMO and LUMO orbitals occurs in alanine 3. This leads to an increased peak intensity at its absorption edge. The strongest peaks occur again in the region of photon energies around 6.5 eV and belong to HOMO − 2 → LUMO transition for alanine 1 and HOMO − 2 → LUMO + 1 transitions for alanines 2 and 3.

Because of the additional sulfur atom, the absorption spectra of the cysteine conformers possess a higher complexity and a larger number of overlapping peaks. Conformer 1 shows the strongest peak at 4.6 eV again due to significantly overlapping HOMO and LUMO orbitals at the carboxyl group. For cysteines 2 and 3, we find HOMO−LUMO transitions at 3.9 and 4.2 eV, respectively, with decreasing peak intensity. The strong peaks around 6.5 eV belong to HOMO − 3 → LUMO transitions. In the case of cysteine 1, this transition already occurs at 6.0 eV with a lower peak intensity. However, the cysteine conformers 1 and 3 with the thiol group pointing in the direction of the carboxyl group yield other strong peaks around 7.7 eV. They are governed by higher optical transitions, for example, HOMO − 4 → LUMO + 1 for cysteine 1 and HOMO − 4 → LUMO + 2 for cysteine 3. Cysteine 2 with the thiol group pointing in the direction of the amino group shows at the energy of 7.7 eV a peak of much lower intensity, which is related to a HOMO − 6 → LUMO transition.

To distinguish between the conformers of the amino acids with more complex side groups, a combination of peaks at the absorption edge and such in the higher frequency region (≈7−9 eV) in the vacuum UV should be used for identification of the conformer.

IV. Summary and Conclusions

For the three most stable conformers of the amino acids glycine, alanine, and cysteine, we have studied the lowest single-electron and electronic pair excitation energies in the framework of DFT and the GGA for exchange and correlation. The influence of spin polarization and other XC functionals has also been discussed. In the case of the lowest single-particle and pair excitations, the many-particle effects such as QP shifts and electron−hole attraction have been taken into account using the ΔSCF approach. Occupation-constrained DFT calculations allowed us to overcome the restriction to ground-state geometries and vertical transitions. The use of geometries of excited amino-acid molecules yielded lower pair energies and corresponding Stokes shifts between absorption and emission lines. In addition, optical absorption spectra have been presented within the independent particle approximation.

For the investigated nine conformers, we computed vertical IPs of the order of 9 eV. We observed a small decrease along the row glycine, alanine, and cysteine but only a weak dependence on the actual geometry of the conformation. The used method gave extremely small electron affinities in agreement with the observation that for several conformers only temporary anion states exist. The vertical pair excitation energies are much smaller than the ionization energies as a consequence of the large exciton binding energies of about 3.7−4.0 eV. These excitation energies are usually reduced after ionic relaxation in the presence of an electron−hole pair. For alanine, the mini-

mization of the driving Hellmann−Feynman forces and the total energy lead to the fragmentation of the molecules. In the cysteine case, this process is restricted to an intramolecular proton transfer. Consequently, the Stokes shifts for cysteine conformers are larger than those in the case of glycine. The optical absorption spectra exhibit significant differences between the conformers with respect to peak positions and peak strengths. They can be traced back especially to the presence of a O−H···N bridge bond or the distance of the thiol group to the carboxyl group (in the cysteine case).

References and Notes

(1) Berg, J. M.; Tymoczko, J. L.; Stryer, L. *Biochemistry*, 5th ed.; Freeman: New York, 2002.
(2) Pandey, R. R.; Bruque, N.; Alam, K.; Lake, R. K. *Phys. Status Solidi A* **2006**, *203*, R5.
(3) Michalat, X.; Pinaud, F. F.; Bentolila, L. A.; Tsay, J. M.; Doose, S.; Li, J. J.; Sundaresan, G.; Wu, A. M.; Cambhir, S. S.; Weiss, S. *Science* **2005**, *307*, 538.
(4) Alexson, D.; Chen, H.; Cho, M.; Dutta, M.; Li, Y.; Shi, P.; Raichura, A.; Ramadurai, D.; Parikh, S.; Stroscio, M. A.; Vasudev, M. *J. Phys.: Condens. Matter* **2005**, *17*, R637.
(5) Mavrandonakis, A.; Farantos, S. C.; Froudakis, G. E. *J. Phys. Chem B* **2006**, *110*, 6048.
(6) Roman, T.; Diño, W. A.; Nakanishi, H.; Kasai, H. *Eur. Phys. J. D* **2006**, *38*, 117.
(7) Wang, Y.; Iqbal, Z.; Malhotra, S. V. *Chem. Phys. Lett.* **2005**, *402*, 96.
(8) Weinkauf, R.; Schanen, P.; Yang, D.; Soukara, S.; Schlag, W. W. *J. Chem. Phys.* **1995**, *99*, 11255.
(9) Baranov, L. Y.; Schlag, E. W. *Z. Naturforsch.* **1999**, *54a*, 387.
(10) Fairman, R.; Åkerfeldt, K. S. *Curr. Opin. Struct. Biol.* **2005**, *15*, 453.
(11) Weinkauf, R.; Schlag, E. W. *J. Phys. Chem. A* **1997**, *101*, 7702.
(12) Császár, A. G. *J. Am. Chem. Soc.* **1992**, *114*, 9568.
(13) Császár, A. G. *J. Mol. Struct.* **1995**, *346*, 141.
(14) Gronert, S.; O'Hair, R. A. J. *J. Am. Chem. Soc.* **1995**, *117*, 2071.
(15) Nguyen, D. T.; Scheiner, A. C.; Andzelm, J. W.; Sirois, S.; Salahub, D. R.; Hagler, A. T. *J. Comput. Chem.* **1997**, *18*, 1609.
(16) Kaschner, R.; Hohl, D. *J. Phys. Chem.* **1998**, *102*, 5111.
(17) Pacios, L. F.; Gómez, P. C. *J. Comput. Chem.* **2001**, *22*, 702.
(18) Pacios, L. F.; Gálvez, O.; Gómez, P. C. *J. Phys. Chem. A* **2001**, *105*, 5232.
(19) Makov, G.; Payne, M. C. *Phys. Rev. B* **1995**, *51*, 4014.
(20) Neugebauer, J.; Scheffler, M. *Phys. Rev. B* **1992**, *46*, 16067.
(21) Adolph, B.; Furthmüller, J.; Bechstedt, F. *Phys. Rev. B* **2001**, *63*, 125108.
(22) Maul, R.; Ortmann, F.; Preuss, M.; Hannewald, K.; Bechstedt, F. *J. Comput. Chem.* **2007**, accepted for publication.
(23) Kohanoff, J. *Electronic Structure Calculations for Solids and Molecules*; Cambridge University Press: Cambridge, 2006.
(24) Hohenberg, P.; Kohn, W. *Phys. Rev.* **1964**, *136*, B864.
(25) Kohn, W.; Sham, L. J. *Phys. Rev.* **1965**, *140*, A1133.
(26) Neville, J. J.; Zheng, Y.; Brion, C. E. *J. Am. Chem. Soc.* **1996**, *118*, 10533.
(27) Lee, K. T.; Sung, J.; Lee, K. J.; Park, Y. D.; Kim, S. K. *Angew. Chem., Int. Ed.* **2002**, *41*, 4114.
(28) Powis, I.; Rennie, E. E.; Hergenhahn, U.; Kugeler, O.; Bussy-Socrate, R. *J. Phys. Chem. A* **2003**, *107*, 25.
(29) Debies, T. P.; Rabalais, J. W. *J. Electron Spectrosc. Relat. Phenom.* **1974**, *3*, 315.
(30) Klasninc, L. *J. Electron Spectrosc. Relat. Phenom.* **1976**, *8*, 161.
(31) Cannington, P. H.; Ham, N. S. *J. Electron Spectrosc. Relat. Phenom.* **1982**, *32*, 139.
(32) Aflatooni, K.; Hitt, B.; Gallup, G. A.; Burrow, P. D. *J. Chem. Phys.* **2001**, *115*, 6489.
(33) Gohlke, S.; Rosa, A.; Illenberger, E.; Brünning, F.; Huels, M. A. *J. Chem. Phys.* **2002**, *116*, 10164.
(34) Li, P.; Bu, Y.; Ai, H. *J. Phys. Chem. A* **2004**, *108*, 1200.
(35) Herrera, B.; Dolgounitcheva, O.; Zakrezwski, V. G.; Toro-Labbe, A.; Ortiz, J. V. *J. Phys. Chem. A* **2004**, *108*, 11703.
(36) Falzon, C. T.; Wang, F. *J. Chem. Phys.* **2005**, *123*, 214307.
(37) Dehareng, D.; Dive, G. *Int. J. Mol. Sci.* **2005**, *5*, 301.

First-Principle Calculations of Electronic Excitations

J. Phys. Chem. A, Vol. 111, No. 20, 2007 **4377**

(38) Osted, A.; Kongsted, J.; Christiansen, O. *J. Phys. Chem. A* **2005**, *109*, 1430.

(39) Jones, R. O.; Gunnarson, O. *Rev. Mod. Phys.* **1989**, *61*, 689.

(40) Godby, R. W.; White, I. D. *Phys. Rev. Lett.* **1998**, *80*, 3161.

(41) Preuss, M.; Schmidt, W. G.; Seino, K.; Furthmüller, J.; Bechstedt, F. *J. Comp. Chem.* **2004**, *25*, 112.

(42) Blöchl, P. E. *Phys. Rev. B* **1994**, *50*, 17953.

(43) Kresse, G.; Joubert, D. *Phys. Rev. B* **1999**, *59*, 1758.

(44) Adolph, B.; Furthmüller, J.; Bechstedt, F. *Phys. Rev. B* **2001**, *63*, 125108.

(45) Kresse, G.; Furthmüller, J. *Comput. Mater. Sci.* **1996**, *6*, 15.

(46) Perdew, J. P. In *Electronic Structure of Solids '91*; Ziesche, P., Eschrig, H., Eds.; Akademie-Verlag: Berlin, 1991.

(47) Perdew, J. P.; Chevary, J. A.; Vosko, S. H.; Jackson, K. A.; Pederson, M. R.; Singh, D. J.; Fiolhais, C. *Phys. Rev. B* **1992**, *46*, 6671.

(48) Burke, K.; Ernzerhof, M.; Perdew, J. P. *J. Chem. Phys.* **1996**, *105*, 9982.

(49) Heyd, J.; Scuseria, G. E.; Ernzerhof, M. *J. Chem. Phys.* **2003**, *118*, 8207.

(50) Perdew, J. P.; Zunger, A. *Phys. Rev. B* **1981**, *23*, 5048.

(51) Hahn, P. H.; Schmidt, W. G.; Bechstedt, F. *Phys. Rev. B* **2005**, *72*, 245425.

(52) Gutowski, M.; Skurski, P.; Simons, J. *J. Am. Chem. Soc.* **2000**, *122*, 10159.

(53) Fuchs, F.; Furthmüller, J.; Bechstedt, F.; Shiskin, M.; Kresse, G. arXiv:cond-mat/0604447, 2006.

(54) Muscat, J.; Wander, A.; Harrison, N. M. *Chem. Phys. Lett.* **2001**, *342*, 397.

(55) Heyd, J.; Scuseria, G. E. *J. Chem. Phys.* **2004**, *121*, 1187.

(56) Weissker, H.-C.; Furthmüller, J.; Bechstedt, F. *Phys. Rev. B* **2002**, *65*, 165328.

(57) Fahrni, C. J.; Henary, M. M.; VanDerveer, D. G. *J. Phys. Chem. A* **2002**, *106*, 7655.

(58) Groth, G.; Jung, W. *FEBS Lett.* **1995**, *358*, 142.

(59) Nir, E.; Janzen, C.; Imhof, P.; Kleinermanns, K.; de Vries, M. S. *Phys. Chem. Chem. Phys.* **2002**, *4*, 732.

(60) Rini, M.; Magnes, B. Z.; Pines, E.; Nibbering, E. T. J. *Science* **2003**, *301*, 349.